20th Australasian Fluid Mechanics Conference
Perth, Australia
5-8 December 2016

Plasma flow simulation using the two-fluid model

D. M. Bond[1], V. Wheatley[1] and R. Samtaney[2]

[1]School of Mechanical and Mining Engineering
The University of Queensland, St Lucia, Queensland 4072, Australia

[2]Mechanical Engineering
King Abdullah University of Science and Technology, Thuwal, Saudi Arabia

Abstract

The interactions between a plasma and magnetic field are of great interest to the astrophysics and fusion power communities and may be modeled under a wide range of simplifying assumptions. Here, we investigate the fully electromagnetic ideal two-fluid plasma model and compare results with the ideal magneto-hydrodynamic (MHD) model. In contrast to the MHD approach the two fluid-model simulates ions and electrons separately, allowing the assumptions of quasi-neutrality, small Larmor radius and small Debye length to be discarded. A two dimensional numerical method has been developed which draws on adaptive spatial resolution and locally implicit time stepping to allow for efficient simulation of the two-fluid plasma model. The Kelvin-Helmholtz instability, with background magnetic field, is simulated over a wide range of plasma regimes. Comparison with hydrodynamic and MHD solutions demonstrates the ability of the two fluid model to bridge the gap between these limiting solutions. The two fluid solutions also demonstrate various stages in the suppression of the Kelvin-Helmholtz instability due to the presence of a background magnetic field.

Introduction

A plasma is a gas that has undergone significant ionisation and is thus composed of its constituent parts, ions, electrons and neutrals. The presence of an electromagnetic field, whether imposed or self generated, can thus influence the motion of the plasma through interaction with the charged particles. An often used model for describing the interaction between a plasma and a magnetic field is the magneto-hydrodynamic (MHD) model. This covers the regime where the motion of the ions and electrons are exactly coupled, allowing no charge separation, leading to the gas behaving like an electrically conducting fluid. At the other end of the spectrum, where there is little interaction between plasma species and velocity space is dominated by anisotropic behaviour, the most suitable approach is to model the plasma through kinetic theory and the collisionless Boltzmann equation. There is also the case when the plasma length scales are so large, in comparison to the characteristic length scale, that there is essentially no electromagnetic effects and the plasma behaves like a neutral fluid. In the intermediate regime we have plasma species of varying charge that may interact, strongly or weakly, via the electromagnetic fields. Depending on the assumptions that are made, various plasma models may be developed that inhabit this intermediate space between the MHD and hydrodynamic or kinetic approximations. In this case the ideal two-fluid model is adopted which retains a finite speed of light along with charge separation effects.

Two-fluid model equations

The equations that make up the two-fluid model are the Euler equations, with additional source terms, and Maxwell's equations of electromagnetism. However, in this paper we will only present the non-dimensional form that was used to generate the presented results.

Non-dimensionalisation

The particular non-dimensional form used herein is given following the definition of various reference parameters shown in table 1.

Name	Definition	Name	Definition
Length	x_0	Charge	q_0
Speed	u_0	Mass	m_0
Magnetic field	B_0	Number density	n_0

Table 1: Non-dimensionalising reference parameters

The non-dimensional variables are then given as follows,

$$\hat{\rho} = \frac{\rho}{m_0 n_0}, \qquad \hat{\vec{U}} = \frac{\vec{U}}{u_0}, \qquad \hat{\varepsilon} = \frac{\varepsilon}{m_0 n_0 u_0^2}, \tag{1}$$

$$\hat{p} = \frac{p}{m_0 n_0 u_0^2}, \qquad \hat{\mathbf{B}} = \frac{\mathbf{B}}{B_0}, \qquad \hat{\mathbf{E}} = \frac{\mathbf{E}}{c B_0}, \tag{2}$$

$$\hat{c} = \frac{c}{u_0}, \qquad \hat{t} = t\frac{u_0}{x_0}, \qquad \hat{q} = \frac{q}{q_0}. \tag{3}$$

Plasma properties

The interaction between plasma species, α, and the electric, $\hat{\mathbf{E}}$, and magnetic, $\hat{\mathbf{B}}$, fields is governed by the Larmor radius, d_L, and Debye length, d_D, which are given in non-dimensional form according to,

$$\hat{d_L} = \frac{d_L}{x_0} = \frac{u_0 m_0}{q_0 B_0 x_0}, \tag{4}$$

$$\hat{d_D} = \frac{d_D}{x_0} = \sqrt{\frac{u_0^2 \varepsilon_0 m_0}{x_0^2 n_0 q_0^2}}. \tag{5}$$

Note that these parameters may be specified for each species. When used in the governing equations they are given with respect to the reference parameters, typically for the ion species. The Larmor radius reflects the degree of interaction between charged particles and the electromagnetic fields while the Debye length may be used as an indication of the degree of charge separation.

Euler equations

The Euler equations for an ideal gas, with specific heat ratio of γ, are given for each species according to,

$$\frac{\partial \hat{\rho}_\alpha}{\partial \hat{t}} + \hat{\nabla} \cdot \left(\hat{\rho}_\alpha \hat{\vec{U}}_\alpha \right) = 0, \tag{6}$$

$$\frac{\partial \hat{\rho}_\alpha \hat{\vec{U}}_\alpha}{\partial \hat{t}} + \hat{\nabla} \cdot \left(\hat{\rho}_\alpha \hat{\vec{U}}_\alpha \hat{\vec{U}}_\alpha + \hat{p}_\alpha \mathbf{I} \right) = \frac{\hat{\rho}_\alpha \hat{r}_\alpha}{\hat{d}_L} \left(\hat{c} \hat{\mathbf{E}} + \hat{\vec{U}}_\alpha \times \hat{\mathbf{B}} \right), \tag{7}$$

$$\frac{\partial \hat{\varepsilon}_\alpha}{\partial \hat{t}} + \hat{\nabla} \cdot \left((\hat{\varepsilon}_\alpha + \hat{p}_\alpha) \hat{\vec{U}}_\alpha \right) = \frac{\hat{\rho}_\alpha \hat{r}_\alpha \hat{c}}{\hat{d}_L} \hat{\vec{U}}_\alpha \cdot \hat{\mathbf{E}}, \tag{8}$$

where

$$\hat{r}_\alpha = \frac{\hat{q}_\alpha}{\hat{m}_\alpha}, \qquad \hat{\varepsilon}_\alpha = \frac{\hat{p}_\alpha}{\gamma - 1} + \frac{\hat{\rho}_\alpha \hat{\vec{U}}_\alpha \cdot \hat{\vec{U}}_\alpha}{2}, \tag{9}$$

and $\mathbf{I}$ is the identity tensor. Note that the coupling with the electromagnetic fields is accomplished via the source terms, the strength of which are governed by the Larmor radius and Debye length, as defined earlier.

Maxwell's equations

The electromagnetic fields are evolved according to Maxwell's equations, given here in non-dimensional form,

$$\frac{\partial \hat{\mathbf{E}}}{\partial \hat{t}} - \hat{c} \hat{\nabla} \times \hat{\mathbf{B}} = -\frac{\hat{d}_L}{\hat{d}_D^2 \hat{c}} \sum_\alpha \hat{\rho}_\alpha \hat{r}_\alpha \hat{\vec{U}}_\alpha, \quad \hat{\nabla} \cdot \hat{\mathbf{B}} = 0, \tag{10}$$

$$\frac{\partial \hat{\mathbf{B}}}{\partial \hat{t}} + \hat{c} \hat{\nabla} \times \hat{\mathbf{E}} = 0, \qquad \hat{\nabla} \cdot \hat{\mathbf{E}} = \frac{\hat{d}_L}{\hat{d}_D^2 \hat{c}} \sum_\alpha \hat{\rho}_\alpha \hat{r}_\alpha. \tag{11}$$

Coupling with the species evolution equations is again through source terms with their influence dictated by the plasma regime.

To enable comparison between the magnetohydrodynamic and two-fluid plasma models, the magnetic field interaction parameter, β, was used. Due to the specific non-dimensionlisation used for the two-fluid equations there must be a two-fluid specific form of this parameter. The MHD and two-fluid values for β are thus given according to

$$\beta_{\mathrm{MHD}} = \frac{2\hat{p}}{\hat{B}^2}, \qquad \beta_{\mathrm{2F}} = \frac{\hat{d}_L^2}{\hat{d}_D^2} \frac{2\hat{p}}{\hat{c}^2 \hat{B}^2}. \tag{12}$$

Implementation

In order to solve this coupled system of equations at high effective resolutions in reasonable time the adaptive mesh refinement (AMR) framework Chombo [2] was used. The base numerical method consists of finite volume scheme with two stage second order Runge-Kutta time integrator [4] with van Leer limited interface values for flux calculation. The two-fluid plasma model is solved with species fluxes calculated according to the HLLC approximate Riemann solver [7] and electromagnetic fluxes calculated from the HLL interface state [3]. The contribution from source terms is solved for locally with the implicit method of Abgrall *et al.* [1]. The MHD solution is obtained for a single species by using an MHD capable HLLE approximate Riemann solver [5, 7] that accounts for the fluid and magnetic field fluxes. The hydrodynamic equations may be solved for with the same method as for the two fluid mode but with the species charge set to zero. The divergence constraints of Maxwell's equations and the MHD equations are enforced through application of the projection method.

Verification

The numerical method was used to simulate a Riemann problem with initial conditions shown in table 2. The plasma regime was set according to $\hat{d}_L = 1/300$ and $\hat{d}_D = \hat{d}_L/100$ with $\hat{c} = 100$ and $\hat{m}_e/\hat{m}_i = 1/1836$. The simulation domain was discretised with a uniform grid of 1024 cells over a domain of $0 \leq \hat{x} \leq 1$ with results shown at a time of $\hat{t} = 0.1$ in figure 1. The solution shows that the numerical method is able to reproduce the solution by Loverich [6] with all features of the combined density profile being captured, albeit with lower numerical dissipation. This implementation of the two-fluid plasma model is thus suitable for further work.

Variable	$x < 1/2$	$x \geq 1/2$
$\hat{\rho}_i$, $\hat{\rho}_e$	1, $\hat{m}_e/\hat{m}_i$	0.125, 0.125 $\hat{m}_e/\hat{m}_i$
$\hat{\vec{U}}$	0	0
$\hat{p}$	0.5	0.05
$\hat{\mathbf{B}}$	$(0.75, 1, 0)^T$	$(0.75, -1, 0)^T$
$\hat{\mathbf{E}}$	0	0

Table 2: Riemann problem initial conditions.

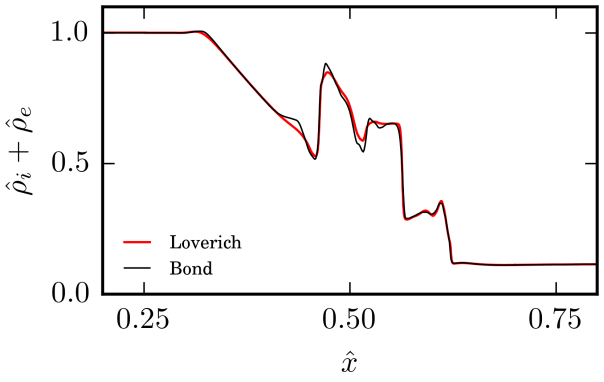

Figure 1: One dimensional combined density profile.

Results

The results to be presented herein are for the Kelvin-Helmholtz instability (KHI). The computational domain was $-1/2 \leq x \leq 1/2$ and $-50 \leq y \leq 50$ with a square Cartesian mesh having an effective resolution of 512 cells across the domain. The domain was periodic in x and had extrapolating boundary conditions in y. The initial flow field had uniform total pressure, $\hat{p} = 1$, and density given by the species mass, $\hat{\rho} = \hat{m}$. For the MHD case $\hat{\rho} = 1$. The velocity field for all species was given by,

$$U_x = U_{x,0} \tanh\left(\ln 39 \frac{x}{a} \right), \quad U_y = U_{y,0} \sin(\phi 2\pi x) \, 2^{-(x/b)^2}, \tag{13}$$

where $U_{x,0}$ was the x-velocity on either side of the shear layer and $U_{y,0}$ was the perturbation velocity of wavenumber ϕ. The widths of the shear layer and velocity perturbation were given by a and b and defined as the distance between symmetric points on a function that cover 95% of the maximum variation.

Simulations were carried out with $U_{x,0} = U_{y,0} = 0.5k$, $a = 0.05$, $b = 0.1$ and $\phi = 2$. The value for k was set by the sound-speed of the primary species (ions). The magnetic field was defined to lie parallel to the shear layer with $\beta_{\mathrm{MHD}} = \beta_{\mathrm{2F}} = 8$. For

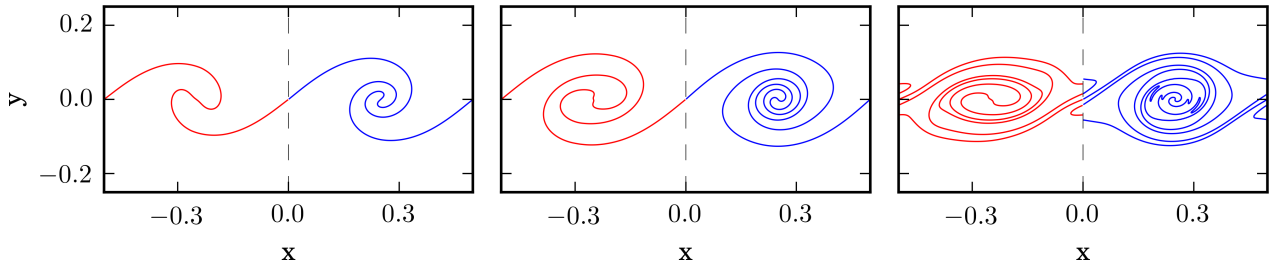

Figure 2: Hydrodynamic KHI ion ($x < 0$) and electron ($x > 0$) interface for $\hat{t} = 0.6$, $\hat{t} = 1.0$ and $\hat{t} = 2.0$.

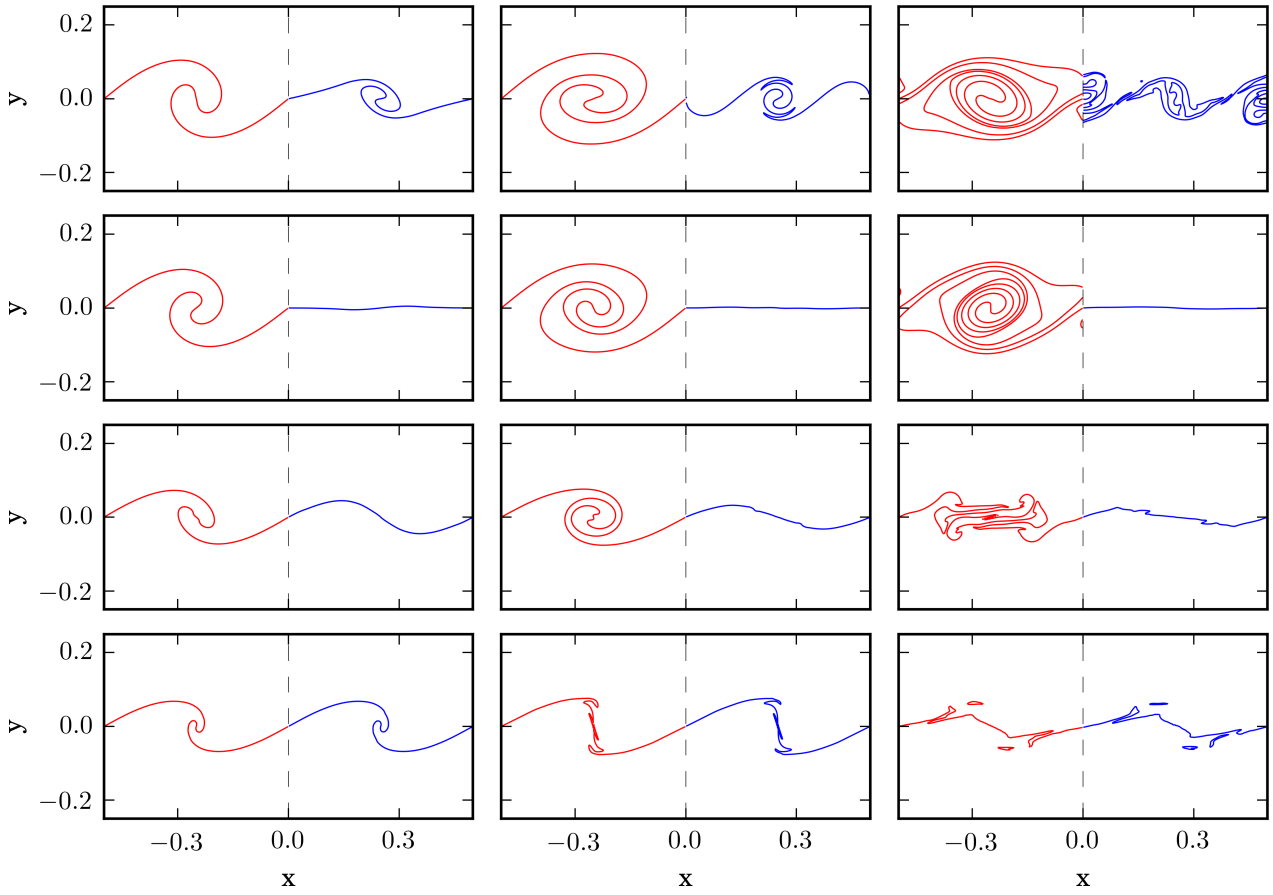

Figure 3: Two-fluid KHI interface location for ions ($x < 0$) and electrons ($x > 0$). Columns show solutions at $\hat{t} = 0.6, 1.0, 2.0$. Rows show $\hat{d_L} = \hat{d_D} = 0.1, 0.01, 0.001, 0.0001$

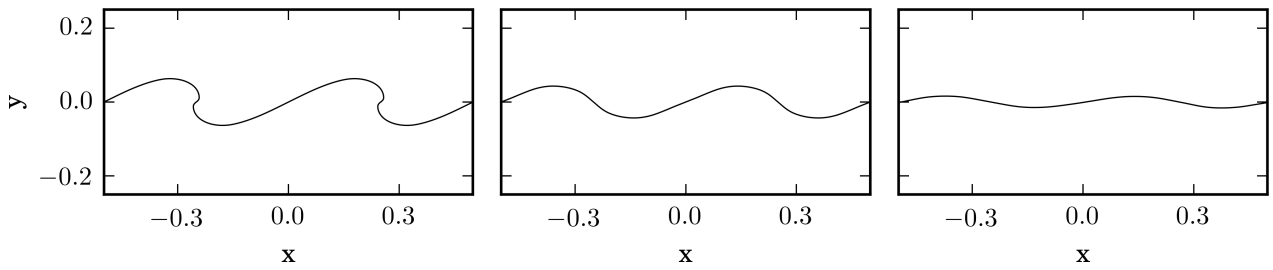

Figure 4: Magnetohydrodynamic KHI interface for $\hat{t} = 0.6$, $\hat{t} = 1.0$ and $\hat{t} = 2.0$.

the two-fluid simulations the Larmor radius and Debye length were varied according to $0.0001 \leq \hat{d}_L, \hat{d}_D \leq 0.1$ with a non-dimensional light speed of $\hat{c} = 50$. The mass of the ions was set to $\hat{m}_i = 1$ and electrons $\hat{m}_e = 0.01$, the species charge was $\hat{q}_i = -\hat{q}_e = 1$. To aid with visualising the evolution of the KHI a passive scalar was defined that allowed tracking of the initial $U_x = 0$ interface. It is this interface that will be shown in figure 2 to figure 4.

Hydrodynamic

The solution of the hydrodynamic case consisted of the Euler solution for two independent fluids. Each fluid was defined exactly as for the two fluid case but with a charge of zero. Figure 2 shows the interface location for the heavy (ion) and light (electron) species. It may be seen that the light species exhibits accelerated roll-up. The simulation was terminated at a time of $\hat{t} = 2$ just prior to significant interaction between the two rollers.

Two-fluid

The introduction of charge to each of the species then allows for interaction with both the self generated electromagnetic and initial magnetic field. The first simulation with two-fluid effects, shown in the first row of figure 3, was with large $\hat{d}_L$ and $\hat{d}_D$ leading to relatively weak interaction between the fields and the species as well as between the species themselves. Minimal changes are thus observed in the ion interface structure, compared to the hydrodynamic case, while there are significant changes to the electron interface. It is evident that the ions are less affected by the fields than the electrons, as expected due to their disparity in momentum, with little correlation between the two species.

With a decrease in $\hat{d}_L$ and $\hat{d}_D$ to 0.01, shown in the second row of figure 3, there was a a marked increase in the effect of the electromagnetic field on the electrons leading to complete suppression of the electron KHI. The ion species was still only mildly affected, with the characteristic roll-up of the interface still evident. It is apparent that the strength of interaction between the species was not yet sufficient for the electrons to have much influence over the ions. This result also shows that the differences in species interfaces indicates that for a given magnetic field strength the suppression of the KHI within each species is heavily dependent on the plasma parameters.

The solution with $\hat{d}_L = \hat{d}_D = 0.001$, shown in the third row of figure 3, shows a significant change. It is evident that the coupling strength has increased to the point where the ion interface structure is being somewhat imposed upon the electrons, the interface is no longer almost flat, while the flattening influence of the electrons is being felt in the ion species. The final frame of this sequence also shows a collapse of the roller structure that has been present in the ions for previous plasma parameters.

Setting $\hat{d}_L = \hat{d}_D = 0.0001$ further increases the strength of coupling between the two species with the interface structure shown to be nearly identical for the time slices shown in the final row of figure 3. The electron and ion species both exhibit the same degree of KHI suppression with a roller being allowed to form before being forced back by the action of the imposed magnetic field. The final interface is not a clean one however, with smaller scale features introduced around the location of the initial vertical velocity perturbations.

Magnetohydrodynamic

The final result, shown in figure 4, illustrates the MHD solution to the KHI problem. This is the solution that could be expected from the two-fluid system of equations in the limit of small Larmor radius and Debye length. The interface shows some initial roll-up, but this is soon reversed by the action of the magnetic field, resulting in a smooth interface at final time. This solution does not show any of the small scale features present in the two-fluid simulations with small plasma parameters.

Discussion & Conclusion

Taking the series of solutions shown in figure 2, figure 3 and figure 4, a progression from completely un-suppressed KHI, to moderately suppressed KHI, may be observed. As the plasma parameters are varied in the two-fluid simulations there appears to be three distinct stages; 1) the electron KHI is fully suppressed, 2) interaction between the species increases with decreased KHI in the ions and a reversion from the fully suppressed electron KHI, and 3) nearly complete correlation between species and moderate suppression of both species KHI. The two-fluid results also show a progression towards the MHD solution, as expected, although higher frequency disturbances in the flow detract somewhat from this.

Finally, it has been shown in this work that it is practical to solve the two-fluid plasma model with physical parameters approaching that of reality. This model has also shown the ability to bridge the transition between pure hydrodynamics, $\hat{d}_L = \hat{d}_D = \infty$, and the MHD limit, $\hat{d}_L = \hat{d}_D = 0$. The use of a magnetic field to suppress the plasma KHI was also demonstrated and shown to depend on the plasma regime, with the electron and ion KHI being suppressed to varying degrees throughout the range of tested values.

Acknowledgements

The work was supported by the KAUST office of Competitive Research Funds under Award No. URF/1/1394-01. V. Wheatley was supported by an Australia Research Council Discovery Early Career Researcher Award (project number DE120102942).

References

[1] Abgrall, R. and Kumar, H., Robust finite volume schemes for two-fluid plasma equations, *Journal of Scientific Computing*, **60**, 2014, 584–611.

[2] Adams, M., Colella, P., Graves, D. T., Johnson, J., Keen, N., Ligocki, T. J., Martin, D. F., McCorquodale, P., Modiano, D., Schwartz, P., Sternberg, T. and Straalen, B. V., Chombo software package for AMR applications - design document, Technical Report LBNL-6616E, Lawrence Berkeley National Laboratory, 2015.

[3] Einfeldt, B., On Godunov-type methods for gas dynamics, *SIAM Journal on Numerical Analysis*, **25**, 1988, 294–318.

[4] Gottlieb, S., Shu, C.-W. and Tadmor, E., Strong stability-preserving high-order time discretization methods, *SIAM Review*, **43**, 2001, 89–112.

[5] Li, S., An HLLC Riemann solver for magneto-hydrodynamics, *Journal of Computational Physics*, **203**, 2005, 344 – 357.

[6] Loverich, J., *A finite volume algorithm for the two-fluid plasma system in one dimension*, Master's thesis, University of Washington, 2003.

[7] Toro, E. F., Spruce, M. and Speares, W., Restoration of the contact surface in the HLL-Riemann solver, *Shock Waves*, **4**, 1994, 25–34.